Deposition of silver nanoparticles on polyvinyl alcohol film using electron beam evaporation and its application as a passive saturable absorber

M.Q. Lokman[a], S.F.A.Z. Yusoff[b], F. Ahmad[a], R. Zakaria[b], H. Yahaya[a], S. Shafie[c,*], R.M. Rosnan[d], S.W. Harun[e]

[a] Malaysia-Japan International Institute of Technology, Universiti Teknologi Malaysia, Kuala Lumpur, Malaysia
[b] Photonics Research Centre, University of Malaya, Kuala Lumpur, Malaysia
[c] Institute of Advanced Technology, Universiti Putra Malaysia, Serdang, Selangor Darul Ehsan, Malaysia
[d] Jeol (Malaysia) Sdn. Bhd, Petaling Jaya, Selangor Darul Ehsan, Malaysia
[e] Department of Electrical Engineering, Faculty of Engineering, University of Malaya, Kuala Lumpur, Malaysia

A B S T R A C T

This study investigated the generation of Q-switched pulse in fibre laser operation at 1550 nm wavelength region using silver nanoparticles (Ag NPs) as passive saturable absorber (SA). The Ag NP SA was prepared through the electron beam evaporation method with a thickness of 10 nm on pure polyvinyl alcohol (PVA) film. The average size of the Ag NPs was around 50 nm and the existence of silver element had been investigated by using the energy dispersive spectroscopy (EDS) technique. The modulation depth of the developed silver-based passive SA was 19% with saturation intensity of 170.26 mW/cm^2. The laser was operated at 1560 nm centre wavelength with 3 dB spectral bandwidth of 1.3 nm. The pulsed laser was able to generate pulse energy of 146.4 nJ with peak power of 20.5 mW at a maximum pump of 90.4 mW. A signal-to-noise ratio (SNR) value of 67.5 dB was obtained at the repetition rate of 65.4 kHz for maximum input pump power.

Introduction

Noble metal nanoparticles (NPs), including gold (Au), silver (Ag), and copper (Cu), have garnered vast attention, especially in the photonics field, due to their attractive optical properties. Metal NPs possess the advantage of broadband saturable absorption induced by surface plasmonic resonance (SPR) from visible to infrared region, which make them suitable to be applied as SA for pulse fibre laser generation at various wavelength operations [1,2], although they are highly influenced by the size, shape, and dielectrics of NPs [3]. Besides, metal NPs have large third-order nonlinearity, especially gold (Au), when compared to graphene or carbon nanotubes [4]. Third-order nonlinearity is responsible for the absorption properties that are important for the change of light that propagates via SA [5]. Rapid growth in the SA technologies from dyes to two-dimensional (2D) materials is almost parallel with the advancement of the fibre laser itself. 2D materials, such as graphene [6], topological insulators [7,8], transition metal dichalcogenides [9], and black phosphorus [10] utilise bandgap size as an important characteristic for SA selection to determine the absorption ability at a desired operation wavelength range. In the case of 2D materials [11], the saturable absorption of photons occurs with energy larger than the respective SA bandgap energy at high intensity that generates an electron-hole interaction. The SA with larger bandgap and weak electron-hole interaction is introduced due to long distance

conduction and valance band separation [11]. Nevertheless, in metal NPs, there are two possibilities of saturable absorption [1]. One is the intensity-dependent shift of the plasmon resonance that leads to strong saturation behaviour [12], while the other refers to the ground state plasmon bleaching related to intrinsic electron dynamics [13].

Several studies have investigated Ag NP as an SA for 1550 nm fibre-pulsed generation. Ahmad et al., reported a Q-switched EDFL by sandwiching the SA between the fibre ferrules [14]. Besides, Ahmad et al. also reported the silver-based passive SA at less than 2 μm region using Thulium-doped fibre as a gain medium [15]. The Ag NP SA was prepared by mixing the Ag NP with methyltrimethoxylane (MTMS) as the host polymer [14]. The saturable absorption of the Ag NP SA was reported at around 31.6%, indicating that the Ag NP embedded in MTMS displayed high potential to serve as SA [14]. The stable pulse started at a relatively low pump power threshold with maximum pulse energy of 8.17 nJ [14]. Guo et al. proposed a Q-switched laser using photodeposition techniques [16]. The Ag NPs were prepared by using the solvothermal reduction method and fibre connector was immersed in the Ag NP aqueous solution for 5 min. The saturable absorption of the SA was approximately 18.5%. The Q-switched pulsed laser was generated at low pump power of 19.9 mW with pulse energy of 133 nJ at maximum pump power of 139 mW [16]. Both the aforementioned studies exhibit positive results in terms of short-pulsed width Q-switched generation. Nevertheless, the techniques utilised by Ahmad et al.

[14,15] generate silver sulphide (Ag$_2$S) due to usage of sulphuric acid in preparing MTMS polymer [17]. Additionally, the optical deposition method reported by Guo et al. [16] suggested low repeatability and required tedious work [18,19].

In this work, Q-switched EDFL was generated by using Ag NP SA. The silver-based passive SA was fabricated via electron beam deposition techniques coated on pure polyvinyl alcohol (PVA) film. Then, the Ag NP SA was deposited in between the fibre ferrules to pulsed fibre laser generation.

Methodology

Fabrication and characterisation of Ag NP SA

The PVA substrate-based film was selected as a supporting polymer in this experiment due to its low optical absorption at 1030 nm and 1558 nm wavelengths. The polyvinyl alcohol (PVA) has high flexibility, high strength, and easy to integrate onto the fibre ferrule [20]. Before depositing the Ag NP on the PVA film, the pure PVA film was prepared by dissolving 1 g of PVA powder (40,000 MW, Sigma Aldrich) into 120 ml of de-ionized (DI) water. At 145 °C, the mixture was stirred until the powder was completely dissolved. Then, 5 ml of PVA solution was carefully poured into a petri dish and left to dry in an ambient condition for 3 days. A thin layer of Ag NP was deposited on the top surface of PVA polymer composites using electron beam evaporation (EB43-T, KCMC). The PVA film was inserted in a vacuum chamber pressurised at 1.0×10^{-4} mbar. Within the stabilised chamber, the filament was turned on at voltage 7 kV and current 120 mA to generate the electron beam. When the constant deposition rate was achieved in 20 min, the main shutter was opened for 5 s to get approximately 10 nm thickness of Ag NP coating. This thickness was controlled by opening the main shutter located inside the vacuum chamber. The fabricated Ag NP SA was kept and sealed in a vacuum bag, and placed in a humid cabinet to prevent Ag oxidation.

The material composition of Ag NP SA was characterised by using Energy-dispersive spectroscopy (EDS), while the surface morphology of Ag NP coated on PVA film was captured by using focused ion beam scanning electron microscopy (FiB-SEM) (Helios Nanolab G3 UC, FEI). A three-dimensional (3D) measuring laser microscope (OLS 4000, Olympus) was used to measure the thickness of PVA film with the deposited silver Nano particles. In order to study the nonlinear optical response of Ag NP SA, balanced twin techniques were carried out. Fig. 1 shows the experimental setup for the nonlinear response measurement. The setup consisted of a self-made mode-locked input source with a repetition rate of 1 MHz and pulse width of 3.41 ps. The mode-locked laser was amplified by using an Erbium-doped amplifier (EDFA). Next, 50% of laser light was tapped out from the Ag NP SA deposited FC/PC fibre ferrule, while another 50% was channelled to the ferrule without SA deposition. The data were collected by constantly reducing the attenuator input, while the output powers of with and without SA were measured using an optical power meter. The curve was fitted by using the transmission fitting equation as given in Eq. (1):

$$Transmission\ Fitting,\ T(I) = 1 - \left[\frac{\alpha_s}{1 + \frac{I}{I_{sat}}} + \alpha_{ns} \right] \tag{1}$$

where α_s is modulation depth, I refers to input intensity, I_{sat} denotes saturation current, and α_{ns} reflects non-saturable absorption.
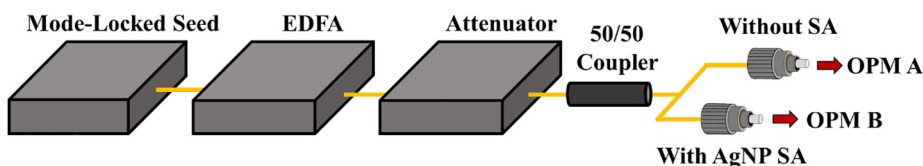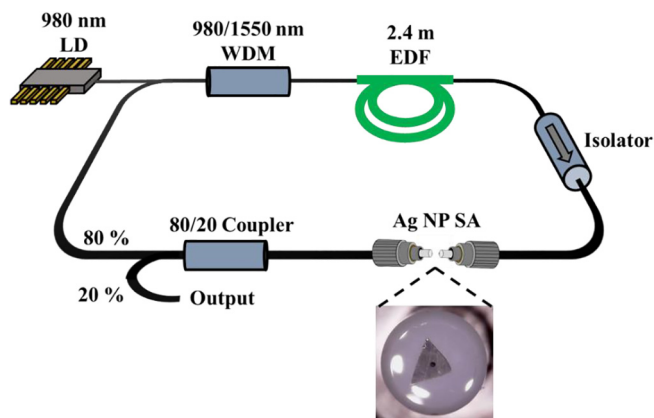

Fig. 2. Experimental setup of the proposed Q-switched fiber laser.

Fibre laser ring cavity setup

Fig. 2 illustrates the ring cavity of the proposed passive Q-switched fibre laser. The cavity was pumped by a 980 nm laser diode with maximum power of 160 mW through wavelength division multiplexing (WDM). A total of 2.4 m Erbium-doped fibre (I-25, FiberCore) with a peak absorption 45 dB/m at 1531 nm was used as the gain medium to generate 1.55 µm region pulse fibre laser. An isolator was employed into the cavity to ensure unidirectional light propagation. The output was tapped out by 80:20 optical coupler, where 80% of light was kept oscillating in the cavity, and the remaining 20% was used for output measurement to observe the pulse train, the signal to noise ratio (SNR), and the optical spectrum. The operating wavelength of the generated pulsed was observed through an optical spectrum analyser (Yokogawa, AQ6370B) with a resolution of 0.02 nm. The pulse train and the SNR were recorded by using 500 MHz Digital Oscilloscope (GW Instek, GDS 3352) and radio frequency spectrum analyser (RFSA) (Anritsu, MS2683A), via 1.2 GHz InGaAs photodetector. The Ag NP SA with the dimension of 1 mm^2 × 1 mm^2 was sandwiched between two FC/PC fibre ferrules and integrated into the ring cavity for pulsed laser generation, as portrayed in Fig. 2. The total length of the laser cavity was approximately 13.4 m.

Results and discussion

In order to verify the presence of silver (Ag) element on PVA, EDS was performed and the analysis is as shown in Fig. 3(a). The high peak of Ag at 3 keV corresponded to high weight percentage of Ag, which was 85.99%. This was followed by carbon (C) and oxygen (O) at weight percentages of 9.44% and 4.57%, respectively, which most probably derived from the host polymer composition (PVA) and the use of carbon for attachment of sample onto the specimen holder. Fig. 3(b) illustrates the image of Ag NP deposited on the PVA film with area of 1 cm^2. The surface morphology of Ag NP on PVA was characterised via FiB-SEM at magnification of 40 kX, as shown in Fig. 3(c). The Ag NPs were composed of several diameters, ranging from 14.28 nm until 171.36 nm with an average diameter of 50.49 nm. The image also portrays the high density and distribution of Ag NP on PVA film without any aggregation. The thickness of the SA, including PVA and Ag NPs, was measured at approximately 55 µm using 3D measuring laser microscope, as shown in Fig. 4.
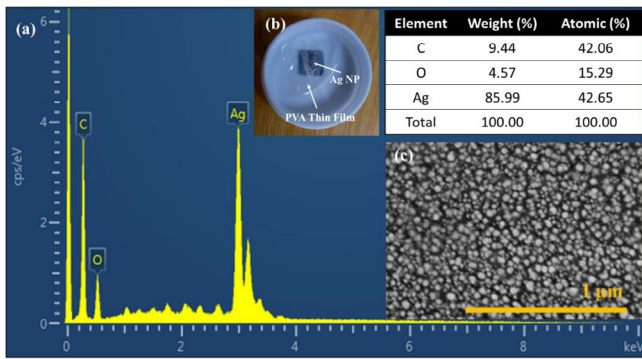

Fig. 1. Twin balanced detector setup for nonlinear transmission analysis of Ag NP SA.

Fig. 3. (a) Energy Dispersive Spectroscopy (EDS) analysis of Ag NP SA, (b) image of Ag NP deposited on the PVA film and (c) is the surface image of Ag NP SA using focused ion beam scanning electron microscopy (FiB-SEM) at magnification 40 kX.
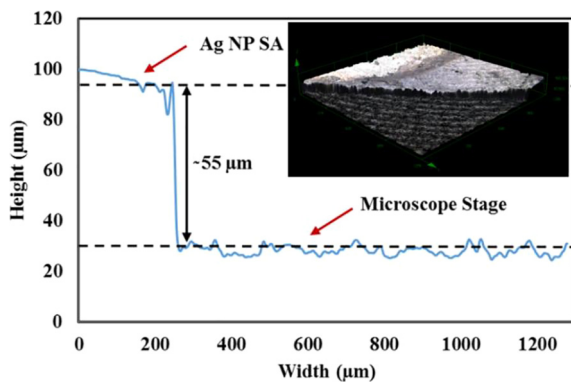

Fig. 4. Thickness measurement using 3D laser microscope. The thickness of the SA is around 55 μm.
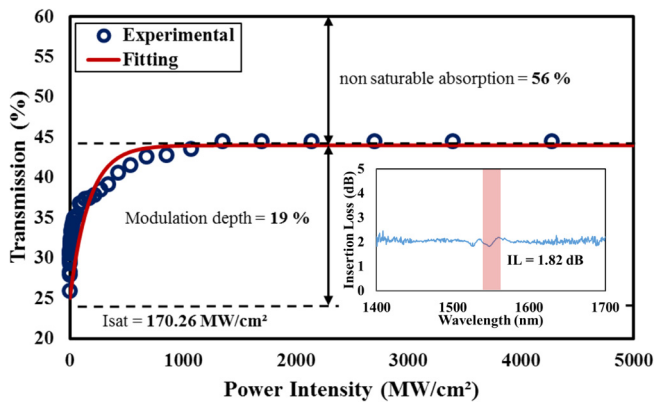

Fig. 5. Nonlinear transmission characteristic of Ag NP SA using twin balanced detector methods and inset is the insertion loss of Ag NP SA using 1550 nm light source.

The nonlinear transmission analysis of Ag NP SA in transmission ratio as a function of power intensity is presented in Fig. 5. By fitting the data from Eq. (1), the modulation depth of the SA was about 19% with non-saturable absorption of 56%. The initial transmission ratio was around 25% and the saturation current of 170.26 MW/cm² was at a transmission ratio of 37.5%. This larger modulation depth was required for a stable Q-switched laser operation and strong pulse shaping [21]. The modulation depth of 19% acquired from this study conforms to those reported in prior studies, such as Guo et al. [16]. The non-saturable absorption of Ag NP was relatively high, most probably due to the low repetition rate of mode-locked pulse laser source that could

induce high power losses by the SAs. This problem can be resolved by using a femtosecond mode-locked source in order to reduce the non-saturable loss. Inset of Fig. 5 shows the insertion loss of the Ag NP SA, which was about 1.82 dB using 1550 nm amplitude spontaneous emission (ASE) light source with input pump power of 40 mW.

The lasing threshold was obtained at 12.7 mW and the stable Q-switched operation was achieved at threshold pump power of 29.4 mW. The low laser threshold displayed low cavity losses in the ring cavity during the continuous wave (CW) operation. In fact, the reported threshold pump power for pulse generation appeared to be lower than the other reported works based on several other materials that served as SAs, such as carbon nanotubes, graphene, and topological insulators [22–25]. The self-started Q-switched operation was also operated at low pump power to indicate that low intensity of light can saturate the electron transition from the valence band to the conduction band. The stable Q-switched pulse train was observed from 29.4 mW until 90.4 mW pump power with decreasing pulse width. The pulses started to get distorted and disappeared when the pump power exceeded 90.4 mW, only to reappear when the pump power was tuned within the range of 29.4 mW until 90.4 mW. This shows that the Ag NP SA was not damaged by the thermal accumulation as it has high damage threshold and the distorted pulse was due to the over-saturation of Ag NP SA at higher pump power [22]. During the experiment, no mode-locking effect was observed. This was probably due to the large cavity loss [26]. The CW was operated at 19.7 mW, while the Q-switched operation was achieved at pump power 29.4 mW. This large difference was due to the loss that suppressed the number of oscillating longitudinal modes, which seemed unfavourable to the mode-locking operation [26].

In order to confirm that the Q-switched pulses were associated to Ag NP, the SA was removed from the ferrule and no pulse was detected even when the pump power was tuned over a wider range. The pure PVA film was tested in the laser cavity and no pulse was generated. This shows that the Ag NP SA was subjected to Q-switched operation. Fig. 6 shows the typical oscilloscope trace of the Q-switched pulse train at 29.4 mW and 90.4 mW. The pulses show asymmetric shape in each envelope and no amplitude modulation can be observed in the pulse train, indicating that the pulse produced was stable. The pulse width at full width at half maximum (FWHM) decreased as the pump power increased, as depicted in the inset of Fig. 6. The shortest pulse width at
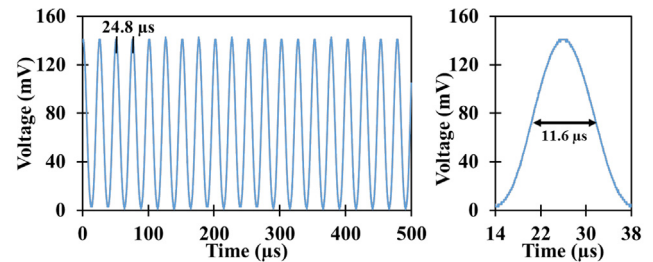
(a)
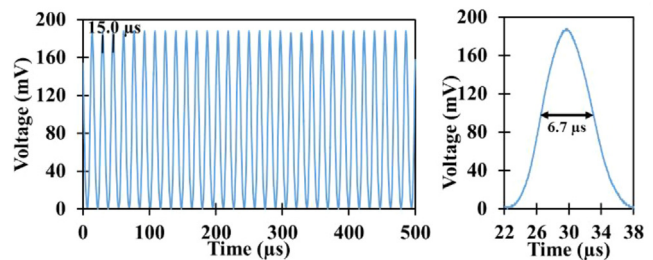
(b)

Fig. 6. Typical pulse train and pulse width at pump power (a) 29.4 mW and (b) 90.4 mW.
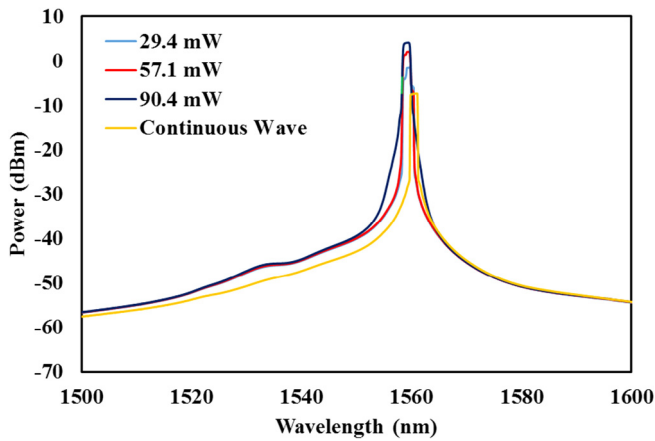
Fig. 7. Optical Spectrum at 29.4, 57.1, and 90.4 mW measured using an optical spectrum analyzer (OSA).

around 6.7 μs was achieved at the maximum pump power of 90.4 mW with pulse-pulse separation of approximately 15.0 μs, which corresponded to the repetition rate of 66.67 kHz. As portrayed in Fig. 6, the separation between two pulses was closer when the pump power increased. Micro-second duration pulse generation can be applied in several applications, such as communications systems, optical sensing, and micromachining [27]. Even shorter pulse duration is desirable for its greater precision and wider applications in these real-world industrial applications.

Fig. 7 illustrates the optical spectrum of CW lasing (without SA) and Q-switched pulses under varied pump power values. The CW lasing was centred at the wavelength of 1560 nm, while the Q-switched laser was operated in the 1558 nm centre wavelength with 3 dB spectral bandwidth of 1.3 nm at maximum pump power of 90.4 mW. The spectrum shifted when the SA was inserted in the laser cavity, indicating that the transition of CW to Q-switching took place due to absorption of light by SA. The nonlinear effects of the fibre and the SA also caused the spectrum broadening to occur. As the Ag NP SA was inserted in the cavity, the spectrum peak increased and slight spectral broadening occurred when the pump power was increased due to reduction in pulse width, which was induced by self-phase modulation (SPM). Fig. 8 portrays the signal to noise ratio (SNR) measured by using radio frequency (RF) spectrum analyser fewer than 500 kHz span. The SNR can be calculated from the difference between peak and pedestal power at the first beat note. The SNR at maximum pump power at a fundamental repetition rate of 65.53 kHz was 67.52 dB. This high SNR indicated that the laser was operated at good stability. Ahmad et al. [14], reported an SNR value of 35 dB, which is lower when compared to the result obtained in this work, using the same starting material of Ag NPs in
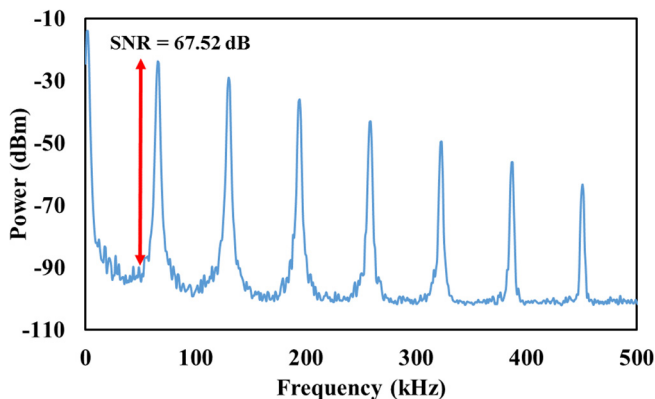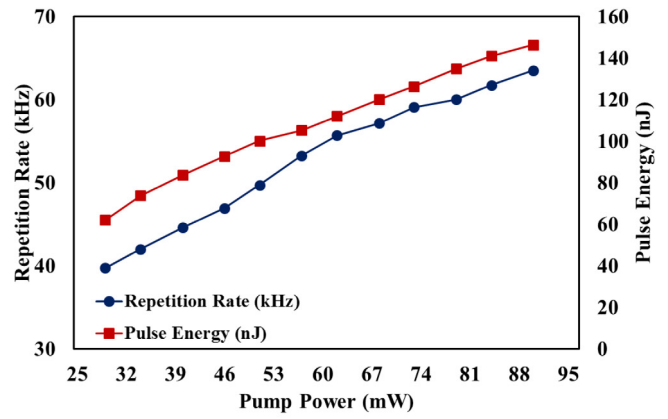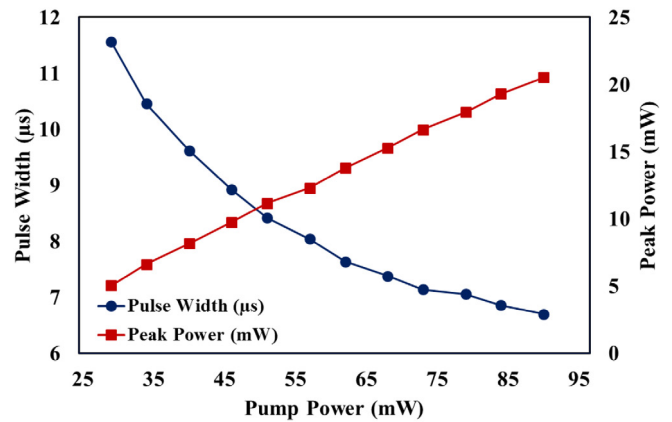

Fig. 8. Radio frequency (RF) spectrum of signal to noise ratio (SNR) measurement at frequency 65.33 kHz with SNR of 67.52 dB.

(a)

(b)

Fig. 9. Relationship between (a) repetition rate and pulse energy, and (b) pulse width and peak power at different pump power.

generating Q-switched laser. No other external frequency component was observed in the RF span, which approved good stability of the laser operation.

Fig. 9(a) illustrates the repetition rate and pulse energy of the Q-switched laser as a function of pump power. The repetition rate was increased from 39.8 kHz to 65.4 kHz as the pump power increased from 29.4 mW to 90.4 mW. The increment of the repetition rates showed that the Q-switching operation can provide frequency tuning by adjusting the level of input pump power. On the other hand, the pulse energy was observed in a linearly increased fashion as the pump power was tuned until the maximum power. At the maximum pump power, the pulse energy was recorded at 146.4 nJ. This high pulse energy was caused by the high modulation depth of Ag NP SA. The high pulse energy was also higher than that reported by Ahmad et al. and Guo et al. [14,16], in fact, considerably higher than most of the works that used SAs based on carbon nanotubes and graphene [24,28,29]. Fig. 9(b) displays the pulse width and the instantaneous peak power as a function of pump power. The pulse widths were reduced from 11.6 μs to 6.7 μs as the pump power increased, showing a typical feature of the Q-switched laser. The value of the shortest pulse width, however, can be further reduced by increasing the modulation depth of the SA, apart from reducing and optimising the overall cavity length to reduce losses. The instantaneous peak power at maximum pump power 90.4 mW was calculated at 20.5 mW.

In the proposed work, Ag NP deposited on PVA using electron beam evaporation appears to generate Q-switched pulsed fibre laser with

Table 1
Result comparison of previous work on AgNP based SA for Q-switched EDFL.

Method	Mod. Depth (%)	Initial Pump Power (mW)	Rep. Rate (kHz)	Pulse Width (µs)	Max Pulse Energy (nJ)	Max Peak Power (mW)	SNR (dB)	Ref
MTMS	31.6	20.0	13.8–39.2	5.9–3.4	~ 4.2	~ 2.0	46.2	[14]
Optical Deposition	18.5	19.9	17.9–58.5	11.4–2.4	132	None	None	[16]
Electron Beam Evaporation	19.0	29.4	39.8–65.4	11.6–6.7	146.7	20.5	67.52	This Work

higher pulse energy and peak power, when compared to prior works based on Ag NP SA. The comparison is presented in Table 1.

Conclusion

As a conclusion, Ag NP coated on the PVA thin film using electron beam evaporation as passive saturable absorber demonstrated and displayed the ability to generate a stable Q-switched pulse at a wavelength of 1550 nm. The diameter of the Ag NP is around 50 nm after being characterised by using FiB-SEM. The high peak of Ag composition in EDS analysis verifies that Ag NP has been successfully deposited on the PVA thin film. Besides, the high modulation depth of 19% proves that Ag NP SA is a good candidate and has high potential to function as saturable absorber. The Ag NPs based passive saturable absorber can generate a pulse at low pump power stably ranging from 29.4 mW up to 90.4 mW. The Q-switched laser operates at the centre wavelength of 1558 nm with 67.52 dB SNR. The laser is also able to achieve high pulse energy of 146.4 nJ with peak power of 20.5 mW.

Acknowledgements

References

[1] Wu D, Lin H, Cai Z, Peng J, Cheng Y, Weng J, Xu H. Saturable absorption of copper nanowires in visible regions for short-pulse generation. IEEE Photonics J 2016;8(4):1–7.

[2] Zheng C, Li W, Chen W, Ye X. Nonlinear optical behavior of silver nanopentagons. Mater Lett 2014;116:1–4.

[3] Jain PK, Huang X, El-Sayed IH, El-Sayed MA. Review of some interesting surface plasmon resonance-enhanced properties of noble metal nanoparticles and their applications to biosystems. Plasmonics 2007;2(3):107–18.

[4] Kang Z, Guo X, Jia Z, Xu Y, Liu L, Zhao D, Qin W. Gold nanorods as saturable absorbers for all-fiber passively Q-switched erbium-doped fiber laser. Opt Mater Express 2013;3(11):1986–91.

[5] Gao Y, Wu W, Kong D, Ran L, Chang Q, Ye H. Femtosecond nonlinear absorption of Ag nanoparticles at surface plasmon resonance. Physica E 2012;45:162–5.

[6] Chu H, Zhao S, Li T, Yang K, Li G, Li D, Hang Y. Dual-wavelength passively Q-Switched Nd, Mg: LiTaO₃ laser with a monolayer graphene as saturable absorber. IEEE J Sel Top Quantum Electron 2015;21(1):343–7.

[7] Ahmad H, Salim MAM, Soltanian MRK, Azzuhri SR, Harun SW. Passively dual-wavelength Q-Switched ytterbium doped fiber laser using selenium bismuth as saturable absorber. J Mod Opt 2015;62(19):1550–4.

[8] Apandi NHM, Ahmad F, Ambran S, Yamada M, Harun SW. Bismuth (III) Telluride (Bi2Te3) based topological insulator embedded in PVA as passive saturable absorber in erbium doped fiber laser. In: IOP Conference Series: Materials Science and Engineering, vol. 210(1), IOP Publishing; 2017. p. 012032.

[9] Mohanraj J, Velmurugan V, Sivabalan S. Transiton metal dichalcogenides based saturable absorbers for pulsed laser technology. Opt Mater 2016;60:601–17.

[10] Rashid FAA, Azzuhri SR, Salim MAM, Shaharuddin RA, Ismail MA, Ismail MF, Ahmad H. Using a black phosphorus saturable absorber to generate dual wavelengths in a Q-switched ytterbium-doped fiber laser. Laser Phys Lett 2016;13(8):085102.

[11] Woodward RI, Kelleher EJ. 2D saturable absorbers for fibre lasers. Appl Sci 2015;5(4):1440–56.

[12] Kim KH, Husakou A, Herrmann J. Saturable absorption in composites doped with metal nanoparticles. Opt Express 2010;18(21):21918–25.

[13] Philip R, Kumar GR, Sandhyarani N, Pradeep T. Picosecond optical nonlinearity in monolayer-protected gold, silver, and gold-silver alloy nanoclusters. Phys Rev B 2000;62(19):13160.

[14] Ahmad H, Ruslan NE, Ali ZA, Reduan SA, Lee CSJ, Shaharuddin RA, Ismail MA. Ag-nanoparticle as a Q switched device for tunable C-band fiber laser. Opt Commun 2016;381:85–90.

[15] Ahmad H, Samion MZ, Muhamad A, Sharbirin AS, Shaharuddin RA, Thambiratnam K, Ismail MF. Tunable 2.0 μm Q-switched fiber laser using a silver nanoparticle based saturable absorber. Laser Phys 2017;27(6):065110.

[16] Guo H, Feng M, Song F, Li H, Ren A, Wei X, Tian J. Q -Switched erbium doped fiber laser based on silver nanoparticles as a saturable absorber. IEEE Photonics Technol Lett 2016;28(2):135–8.

[17] Ezenwa IA, Okereke NA, Egwunyenga NJ. Optical properties of chemical bath deposited Ag₂S thin films. Int J Sci Technol 2012;2(3):101–6.

[18] Martinez A, Fuse K, Xu B, Yamashita S. Optical deposition of graphene and carbon nanotubes in a fiber ferrule for passive mode-locked lasing. Opt Express 2010;18(22):23054–61.

[19] Kashiwagi K, Yamashita S. Optical deposition of carbon nanotubes for fiber-based device fabrication. Frontiers in guided wave optics and optoelectronics. IntechOpen; 2010.

[20] Zhang M, Hu G, Hu G, Howe RCT, Chen L, Zheng Z, Hasan T. Yb-and Er-doped fiber laser Q-switched with an optically uniform, broadband WS₂ saturable absorber. Sci Rep 2015;5:17482.

[21] Chiu JC, Lan YF, Chang CM, Chen XZ, Yeh CY, Lee CK, Cheng WH. Concentration effect of carbon nanotube based saturable absorber on stabilizing and shortening mode-locked pulse. Opt Express 2010;18(4):3592–600.

[22] Yu Z, Song Y, Tian J, Dou Z, Guoyu H, Li K, Zhang X. High-repetition-rate Q-switched fiber laser with high quality topological insulator Bi₂Se₃ film. Opt Express 2014;22(10):11508–15.

[23] Williams RJ, Jovanovic N, Marshall GD, Withford MJ. All-optical, actively Q-switched fiber laser. Opt Express 2010;18(8):7714–23.

[24] Cao WJ, Wang HY, Luo AP, Luo ZC, Xu WC. Graphene-based, 50 nm wide-band tunable passively Q-switched fiber laser. Laser Phys Letts 2011;9(1):54.

[25] Chen Y, Zhao C, Chen S, Du J, Tang P, Jiang G, Tang D. Large energy, wavelength widely tunable, topological insulator Q-switched erbium-doped fiber laser. IEEE J Sel Top Quantum Electron 2014;20(5):315–22.

[26] Luo Z, Huang Y, Zhong M, Li Y, Wu J, Xu B, Weng J. 1-, 1.5-, and 2-μm fiber lasers Q-switched by a broadband few-layer MoS₂ saturable absorber. J Lightw Technol 2014;2(24):4077–84.

[27] Westphäling T. Pulsed Fiber Lasers from ns to ms range and their applications. Phys Procedia 2010;5:125–36.

[28] Dong B, Hu J, Liaw CY, Hao J, Yu C. Wideband-tunable nanotube Q-switched low threshold erbium doped fiber laser. Appl Opt 2011;50(10):1442–5.

[29] Zhou DP, Wei L, Dong B, Liu WK. Tunable passively Q-switched erbium-doped fiber laser with carbon nanotubes as a saturable absorber. IEEE Photonics Technol Lett 2010;22(1):9–11.